JOURNAL OF MECHANICAL ENGINEERING AND SCIENCES
ISSN: 2289-4659 e-ISSN: 2231-8380
VOLUME 17, ISSUE 2, 2023, 9443 – 9452
DOI: https://doi.org/10.15282/jmes.17.2.2023.3.0747

اونيۏرسيتي مليسيا ڤهڠ
UNIVERSITI MALAYSIA PAHANG

RESEARCH ARTICLE

Performance degradation analysis of a medium pressure superheater due to tube deactivation

A.S. Haqim [1,3], W.A.N.W. Mohamed [2,3,*], A.S. Tijani [2,3]

[1] PETRONAS Chemicals Methanol Sdn Bhd, Rancha-Rancha Industrial Estate, 87000, Wilayah Persekutuan Labuan, Malaysia
[2] Efficient Energy Conversion Technologies, College of Engineering, Universiti Teknologi MARA, 40450, Shah Alam, Selangor, Malaysia
Phone: +60355436277
[3] School of Mechanical Engineering, College of Engineering, Universiti Teknologi MARA, 40450, Shah Alam, Selangor, Malaysia

ABSTRACT - Steam is essential in petrochemical industries for the transportation of thermal energy and usage in some reforming process. Superheaters are heat exchangers that convert saturated steam to dry steam by utilizing waste heat from the flue gas stream. Medium pressure steam superheaters are prone to tube deterioration due to service at elevated temperatures and erosion from the presence of liquid phase in the steam, leading to tube plugging after tube failure. This reduces the overall surface heating area of the superheater. Relations between the tube plugging practice and the energy dynamics of the superheaters are important for engineers to identify the responses of the superheater for operation planning, and this issue has not been extensively explored academically. This article analyses the deterioration of superheater performance due to reduction of surface heating area based on operational data of a petrochemical steam generation line. The objective is to find relations between the effect of tube plugging on the states of both steam and flue gas streams, as well as its impact on the overall energy exchange. The operating conditions of a superheater at two separate service years, before (year 2014) and after (year 2017) tube plugging, were compared through the first law energy analysis. The average steam inlet temperatures were between 248 ˚C and 250 ˚C, at flow rates between 70 and 90 ton/hour. The analysis indicated that 0.3 to 0.8 % increase in inlet energy is required for every plugged tube to compensate for the reduction of heating surface. At 3 % reduction of heating surface area, the heat exchanger effectiveness decreases by an average of 11 % that also leads to a lower steam temperature output by approximately 6% from the design operating temperature. These results would assist steam engineers to analyse changes to the energy economics of the whole plant and decide the feasibility of replacing existing superheaters with new ones. Also, another significant finding to be considered by steam engineers is that the current practice of increasing the steam flow rate does not offset the loss of energy effectiveness due to tube plugging.

ARTICLE HISTORY
Received : 03rd Nov. 2022
Revised : 15th Mar. 2023
Accepted : 26th Mar. 2023
Published : 28th June 2023

KEYWORDS
Flue gas
Plugging
Superheater
Steam
Tube deactivation

1.0 INTRODUCTION

An important agenda in sustainability is the efficient use of energy. The projected waste heat from global industries amounts to approximately 33% from the total energy produced. In the United States, around 3000 TWh/year of waste heat was produced (equivalent to 1.72 billion barrels of oil) while in the United Kingdom, the production of waste heat was estimated at 11.4 TWh/year [1]. These level of energy losses exert a great burden on the energy supply chain as well as the environmental health. Sustainable Development Goals require greater energy efficiency practices through a more effective management of energy usage at each step of an industrial process, as this directly contributes to the reduction of fossil fuel consumption and carbon dioxide emission.

Steam is used in mechanical systems as a thermal energy carrier. Boilers are used to produce steam at high temperatures and pressures based on the requirements of a specific process such as heating, drying or expansion in a turbine. In petrochemical industries, superheated steam at temperatures between 750 °C – 875 °C is needed to convert natural gas into its hydrocarbon components through steam reforming in the auto-thermal reactor and primary reformer [2]. The sustainability agenda demands that waste heat recovery is an essential process in a boiler system to increase the energy efficiency, lower the consumption of fossil fuels and reduce the levelized costs of production. Waste heat is categorised as high (above 650 °C), medium (230 °C to 650 °C) and low (lower than 230 °C) [3] grades. Optimisation of energy utilisation is usually performed at each stage of the energy generation and transport processes using mathematical model tools such as the mechanism method, data-driven statistical analysis and mixed mode methods [4].

The efficiency of natural gas boilers ranges from 88% to 93% with flue gas temperatures in the range of 180 °C to 200 °C [5]. Energy recovery technologies for industrial boilers have grown rapidly with the development of heat

***CORRESPONDING AUTHOR | W. A. N. W. Mohamed** | ✉ wanajmi@uitm.edu.my

exchangers that functions as economisers, superheaters and combustion air preheaters. The investment efficacy of these energy recovery devices is usually assessed through the waste heat quality and quantity, as well as on its targeted outputs [6]. The thermal efficiency of these waste heat recovery systems can be improved by increasing the critical temperature of the working fluid or by reducing the temperature difference between the working fluid and the flue gas [7]. Blumberg et al. [8] evaluated the exergy of a methanol-producing plant with natural gas feeds and stated that the exergy destruction calculated from the superheating process alone was 21.7 MW mainly due to the release of gases from the flue gas duct. This indicates that a superheater is a vital component for higher exergy efficiency of the plant.

A superheater is a heat exchanger functioning as a waste heat recovery device to increase the temperature of saturated steam to superheated phase by utilising the heat in a combustion flue gas. The main advantage of using superheater tubes is the reduction of fuel consumption through the recovery of flue gas heat. From a thermodynamic analysis, increasing the pressure of superheaters by 100% would increase the net power of a coal-fired power plant by 8%, while increasing the dry steam temperature from 540 °C to 580 °C (a 7% increase) would lead to a 6% net power increase [9]. High pressure superheated steam harnesses high quality heat from flue gas with temperatures above 650 °C while medium pressure superheated steam produces heat at temperatures ranging from 230 °C to 650 °C [10].

Superheater tubes are reported to be the most common malfunctioning component in boilers. Approximately 40% of forced boiler shutdowns are caused by damages in superheater tubes [11]. High operating temperature is the main reason for frequent failures of the steam superheater due to creep as well as formation of heavy clinkers on the tube surfaces, leading to localised tube overheating and concentrated flue gas flow over a specific zone of the tube bundle [12]. Another root cause of the failure is fire-side corrosion of the tubes due to the use of low-grade fuel that causes continuous scale formation formed from fly ashes. The scales, generally complex alkali sulphates, lead to corrosion and reduction of wall thickness [13]. A drastic reduction in bulk hardness of the tube alloy together with excessive oxidation may result from long-term operational service [14]. The occurrence of long-term tube overheating also increases the chances for coagulation of carbides at both outer and inner regions of the tubes [15]. Injection of cold water into the attemperator to keep steam temperatures below the allowed limit and activation of soot blowers to remove ash deposits from superheater surfaces are also major causes of high tube thermal stresses due to sudden and large changes in temperature [16]. Continuous operation at elevated pressures and temperatures leads to severe tube damage and the reduction of the superheater heating surface. Consequently, the process steam temperature and pressure are negatively affected by the reduction of heating surface [17], unless the temperature differences between the flue gas and steam inlets are minimised to offset the effects of the heat transfer rate [18].

Efficiency analysis for high-temperature thermal systems is usually coupled between the first law and second-law efficiency definitions. The first-law energy analysis does not provide the actual efficiency and thermodynamic losses of a thermal system. Exergy analysis, based on second-law principles of entropy generation, provides a greater detail on the irreversibility of an actual process, or simply known as losses. In a power plant analysis by Aljundi [19], the process contributing to the highest energy loss was identified through exergy analysis. The combustion chamber of the boiler had the highest exergy destruction at 77% with an energy efficiency of 43.8%. Relatively, Kumar [20] reported an 83% exergy destruction in a boiler of a coal-fired power plant. Clay and Mathius [21] reported that the steam generator produced the highest energy destruction in a subcritical pulverized coal power plant. Elhelw et al. [22] confirmed that steam superheaters has a significant effect on the cycle exergy losses and suggested increasing the steam inlet to high pressures to reduce exergy loss. Also, Bianco et al. [23] applied multi-objective optimization to obtain a 20% economic savings while minimizing the size of the steam generator that shows how crucial the process is in a power plant.

Studies that describe and identify cases of superheater failures are popular due to the practical need to understand and act towards preventive maintenance. Begum et al. [24] modelled a failed boiler tube due to creep and proposed an operation optimisation approach to minimise creep damages. Based on an analysis by Movahedi-Rad et al. [15] and Saha et al. [25], the failure of superheater tubes was due to long-term superheating. Ahmad et al. [26] applied the hoop stress method to model the failure of the rear waterwall tube of a boiler, while Botha and Hindley [27] provided a modelling methodology for boiler tube failure. There are studies conducted on tube failure analysis subjected to superheater service life, such as the models on the thermal mechanical fatigue suffered by superheater tubes [28, 29]. Superheaters usually have a service life cycle of 20 years before being replaced where tube damage is a common problem due to service life factor [30]. The current practice to justify the replacement of superheaters is by limiting the allowable tube plug at 10% from the total number of tubes, or a drop-in superheater effectiveness by 10% from its nominal value [31].

The plugging of superheater tubes directly causes heat transfer mechanics deterioration due to the reduction in effective heating surface. Steam engineers usually attempt to offset the loss in heating surface by adjusting the inlet conditions of the steam and flue gas. The mentioned failure analysis of superheater tubes is localised and does not provide information on the dynamic response of the superheater energy balance to the tube failures. However, steam engineers need to have a guidance in properly adjusting the steam flow rates or flue gas temperatures in order to achieve the desired steam quality without significantly offsetting the economics of the boiler operation. Thus, profiling relationships between tube plugging and the energy dynamics of a superheater have been identified as a knowledge gap and it is an important subject for practicing steam engineers to determine new operating settings or decide the severity of the superheater effectiveness deterioration.

This manuscript presents a systematic energy analysis to identify the effects of operating characteristics of a superheater due to tube plugging. There has been no critical literature regarding the changes in the energy dynamics and effectiveness of superheaters after suffering tube failures. Based on the operational data from a steam generation system of a methanol production plant, the energy profiles of the steam superheater were analysed before and after the tube failures occurred. Data sets from year 2014 and 2017 were compared based on the first law of thermodynamic analysis. The objective is to identify the direct effect of tube deactivation on the steam and flue gas streams, the changes to the energy demand, as well as the energy exchange effectiveness. The importance of this study has the potential to assist boiler engineers in predicting the direct impact from the loss of superheater heating surface and to provide an engineering guidance in strategic operation planning.

1.1 Steam Superheater Model

The reference steam superheater for this study is a medium pressure superheater with 132 tubes and a total heating area of 4288 m^2 that has been in service since the year 2004. It is a convection tube type heat exchanger that functions to supply dry superheated steam for the purpose of steam reforming process in a methanol production plant. Figure 1 displays the schematic arrangement of the superheater relative to the reformer, auxiliary boiler and flue gas chimney. The flue gases from both the boiler and the reformer are channelled to the superheater. The waste heat recovery process from the flue gases is multifunctional. The main heat recovery is for the purpose of increasing the steam temperature from the steam drum to produce high quality superheated steam. A secondary function of the waste heat recovery is to preheat the atmospheric air intake before it is channelled as combustion air to the boiler and as heated air to the reformer.

The boundary of the superheater system analysed in this work is also shown in Figure 1 (dashed box). High temperature flue gas is the heat source that transfers its heat to the steam flowing in the tube arrays. The total heating surface has reduced over the years due to tube deactivation. Table 1 lists the active number of tubes in 2014 and 2017. Since its installation, a total of 9 tubes have been plugged due to erosion and corrosion. From 2004 to 2014, 5 tubes were already deactivated, and 4 more tubes were deactivated in 2017. Due to the unavailability of detailed operational data from 2004 to 2014, the period of analysis is limited to the comparison of superheater performance between the years 2014 and 2017, where there is a 3% reduction in heating surface due to the deactivation of four tubes.

Figure 2 displays the condition and morphology of the damaged tubes that usually occur at the tube bends. Tube plugging was conducted at the inlet header. Investigations concluded that the damage was due to the presence of two-phase flow, leading to accelerated corrosion and erosion at the tube bends.

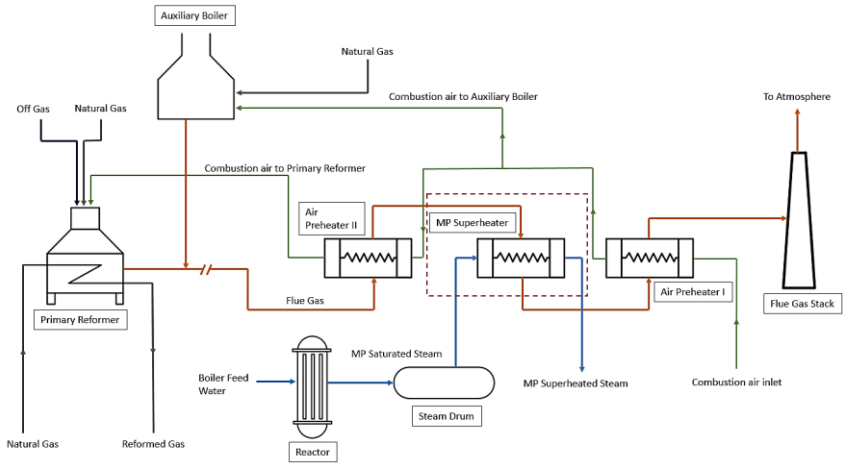

Figure 1. Waste heat recovery system of a methanol production plant

Table 1. The actual tube and surface heating area of the superheater under new (2004) and tube-plugged conditions

Superheater Conditions	2004 (Original Conditions)	2014	2017
Total Active Tubes	132	127	123
Plugged Tubes	0	5	9
Heating Surface Area (m^2)	4288	4126	3996

2.0 MODELLING THE HEAT EXCHANGER EFFICIENCY

Table 3 shows a list of operational data for the steam superheater which was obtained from the data acquisition system for the steam stream and the flue gas stream. The objective of the analytical model is to determine the effects of tube plugging on the changes in the operating condition of the superheater. The parametric changes of concern are the inlet/outlet temperatures of both fluid streams that indicate the fluctuations in energy conversion efficiency of the

superheater. In addition, the analysis also focuses on the actual effects of increasing the steam flow rates to offset the effects of decreasing heating surface that was incorporated during operation.

Actual data was taken during the startup of the superheater after planned shutdown for superheater repairs in 2014 and 2017. A total of 30 sets of data were taken at each 1 tonnes/hr increment of steam mass flow rate starting from 70 tonnes/hr for each year. Operating data of the superheater such as temperature and pressure are extracted from PI Process Book (refer to Table 2), a data collection and storage software used by the plant, and directly linked to the instrumentations.

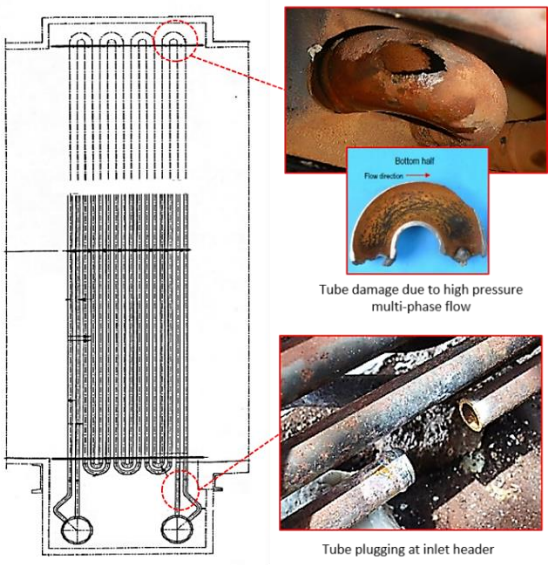

Figure 2. Locations of damaged and plugged tubes of the steam superheater

Table 2. Temperature, pressure and flow indicators in waste heat recovery system

Instrument Label	Description	Unit	Instrument Model
TIAH-1041	Temperature of Superheater Inlet Flue Gas	^{o}C	RÜEGER
TI-1042	Temperature of Superheater Outlet Flue Gas	^{o}C	RÜEGER
TI-1594	Temperature of Inlet Superheater	^{o}C	RÜEGER
TI-1047	Temperature of Outlet Superheater	^{o}C	RÜEGER
PI-1514	Pressure of Inlet Superheater	bar	WIKA
PI-1505	Pressure of Outlet Superheater	bar	WIKA
FI-2008	Mass Flow Rate of Steam	Ton/hr	WIKA
FFIC-1012	Combustion Air to Auxiliary Boiler	Nm^3/hr	WIKA
FFIC-1014	Combustion Air to Auxiliary Boiler	Nm^3/hr	WIKA
FFIC-1016	Combustion Air to Auxiliary Boiler	Nm^3/hr	WIKA
FFIC-1018	Combustion Air to Auxiliary Boiler	Nm^3/hr	WIKA
FIC-1009	Combustion Air to Reformer	Nm^3/hr	WIKA
FIC-1007	Natural Gas Fuel to Reformer	Nm^3/hr	WIKA
FIC-1008	Mixture Gas Fuel to Reformer	Nm^3/hr	WIKA
FICAL-1011	Natural Gas Fuel to Auxiliary Boiler	Nm^3/hr	WIKA
FICAL-1013	Natural Gas Fuel to Auxiliary Boiler	Nm^3/hr	WIKA
FICAL-1015	Natural Gas Fuel to Auxiliary Boiler	Nm^3/hr	WIKA
FICAL-1017	Natural Gas Fuel to Auxiliary Boiler	Nm^3/hr	WIKA
TI-1058	Flue Gas Temperature from Auxiliary Boiler	^{o}C	RÜEGER

2.1 Flue Gas Model

There are no sensors in the flue gas duct to measure the mass flow rate of flue gas. However, there are multiple flow rate meter to measure the volumetric flow rate of the natural gas, mixed gas and combustion air entering both the primary reformer and auxiliary boiler. The superheater is modelled as a steady-flow system where the law of mass conservation dictates that the mass of the flue gas should be equal to the mass entering the combustion system which consists of natural gas fuel, mixed gas fuel and the combustion air [32, 33].

$$\sum \dot{m}_{in} = \sum \dot{m}_{out} \tag{1}$$

$$\dot{m}_{flue\ gas} = \dot{m}_{NG} + \dot{m}_{MG} + \dot{m}_{air} \tag{2}$$

The only available data to calculate the actual mass flow rate of flue gas is the volumetric flow rate of elements for combustion entering the waste heat recovery system. Therefore, to find the mass flow rate of flue gas, the compressibility factor of each gas into the system must be determined. The compressibility factor of the natural gas fuel and gas fuel mixture is determined based on the pseudo reduced temperatures and pressures [34],

$$T_{pr} = \frac{T}{T_{pc}} \tag{3}$$

$$P_{pr} = \frac{P}{P_{pc}} \tag{4}$$

The compressibility factor of gas [34],

$$Z_{gas} = 1 + A_1 P_{pr} + A_2 P_{pr}^2 + \frac{A_3 P_{pr}^{A_4}}{T_{pr}^{A_5}} + \frac{A_6 P_{pr}^{(A_4+1)}}{T_{pr}^{A_7}} + \frac{A_8 P_{pr}^{(A_4+2)}}{T_{pr}^{(A_7+1)}} \tag{5}$$

where the values of $A_1$to A_8 are referred to Table 3 based on the calculated Pseudo Reduced Pressure of the gas.

Table 3. Coefficients for the Pseudo reduced pressure for Eq. (5) [35]

Coefficients	0.01 <P_{pr}< 3.0	3.0 <P_{pr}< 15.0
A_1	0.007698	0.015642
A_2	0.003839	0.000701
A_3	−0.467212	2.341511
A_4	1.018801	−0.657903
A_5	3.805723	8.902112
A_6	−0.087361	−1.136000
A_7	7.138305	3.543614
A_8	0.083440	0.134041

Taking into account the compressibility factor, the mass flow rates of the natural gas fuel and gas fuel mixture can then be calculated using the ideal gas law provided that the gas condition satisfies $P_r < 1$ and $T_r > 2$ [33],

$$P\dot{V} = \frac{Z_{gas}\dot{m}RT}{M} \tag{6}$$

2.2 Combustion Air Model

The compressibility of combustion air was calculated based on the equations used by Ren et al. [36]

$$Z_{air} = \frac{PV_m}{RT} = 1 + \frac{B}{V_m} + \frac{C}{V_m^2} \tag{7}$$

$$B = \frac{(B_r^0(T_r) + \omega B_r^1(T_r) + \theta B_r^2(T_r)) \cdot R \cdot T_C}{P_C} \tag{8}$$

$$C = \frac{(C_r^0(T_r) + \omega C_r^1(T_r) + \theta C_r^2(T_r)) \cdot R \cdot T_C}{P_C} \tag{9}$$

$$B_r^0(T_r) = 0.13356 - \frac{0.30252}{T_r} - \frac{0.15668}{T_r^2} - \frac{0.00724}{T_r^3} - \frac{0.00022}{T_r^8} \tag{10}$$

$$B_r^1(T_r) = 0.17404 - \frac{0.15581}{T_r} - \frac{0.38183}{T_r^2} - \frac{0.44044}{T_r^3} - \frac{0.00541}{T_r^8} \tag{11}$$

$$C_r^0(T_r) = 0.13356 + \frac{0.02432}{T_r^{2.8}} - \frac{0.00313}{T_r^{10.5}} \tag{12}$$

$$C_r^1(T_r) = -0.02676 + \frac{0.0177}{T_r^{2.8}} + \frac{0.04}{T_r^{3}} - \frac{0.003}{T_r^{6}} - \frac{0.00228}{T_r^{10.5}} \tag{13}$$

The ideal gas is used to calculate the mass flow rate of combustion air based on its compressibility factor and conditions where $P_r < 1$ and $T_r > 2$ [33],

$$P\dot{V}_{air} = \frac{Z_{air}\dot{m}_{air}RT}{M_{air}} \tag{14}$$

2.3 Calculation of Specific Heat at Constant Pressure, c_P for Flue Gas

There are no indicators to determine the specific heat at constant pressure, c_P for flue gas. c_P calculation is part of the model for the analysis. The specific heat at constant pressure for the flue gas mixture was determined from the simplified approach by Coskun et al. [37],

$$c_{P,flue\ gas} = \frac{c_{P,C}}{(a_C + b_N + c_H + d_S)} \cdot \frac{m_{tot.\ stoic}}{m_{flue\ gas}} + f_A \tag{15}$$

The total mass flow rate of the reactants at stoichiometric condition, $\dot{m}_{total\ stoic}$

$$\dot{m}_{total\ stoic} = \dot{m}_{fuel} + \dot{m}_{air\ stoic} \tag{16}$$

where the fuel flow rate, $\dot{m}_{fuel}$, is a measured parameter, while the stoichiometric air flow rate, $\dot{m}_{air\ stoic}$, is calculated from

$$\dot{m}_{air\ stoic} = (2.9978 \cdot K_H - 0.3747 \cdot K_O + 0.3747 \cdot K_S + K_C) \cdot (11.445) \tag{17}$$

$$\dot{m}_{flue\ gas} = \dot{m}_{fuel} + \dot{m}_{air} \tag{18}$$

$$\dot{m}_{air} = (2.9978 \cdot K_H - 0.3747 \cdot K_O + 0.3747 \cdot K_S + K_C) \cdot (11.445 \cdot n) \tag{19}$$

$$\dot{m}_{flue\ gas} = (2.9978 \cdot K_H - 0.3747 \cdot K_O + 0.3747 \cdot K_S + K_C) \cdot (11.445 \cdot n) + \dot{m}_{fuel} \tag{20}$$

2.4 Heat Exchanger Effectiveness Analysis

From Cengel [38], the effectiveness, ε of a heat exchanger can be determined by the ratio between the actual and maximum heat transfer rates between the two working fluids,

$$\varepsilon = \frac{\dot{Q}}{\dot{Q}_{max}} = \frac{Actual\ heat\ transfer\ rate}{Maximum\ possible\ heat\ transfer\ rate} \tag{21}$$

from energy balance of the hot and cold fluid streams, the actual heat transfer can be calculated based on

$$\dot{Q} = C_c\left(T_{c,out} - T_{c,in}\right) = C_h\left(T_{h,in} - T_{h,out}\right) \tag{22}$$

where the heat capacity, C, of both fluid streams can be calculated as,

$$C_h = \dot{m}_h c_{p,h} \tag{23}$$

$$C_c = \dot{m}_c c_{p,c} \tag{24}$$

The maximum heat transfer rate is dependent on the maximum temperature difference in the heat exchanger, while C_{min} is the lower value of heat capacity between the two fluid streams,

$$\Delta T_{max} = T_{h,in} - T_{c,in} \tag{25}$$

$$\dot{Q}_{max} = C_{min}\left(T_{h,in} - T_{c,in}\right) \tag{26}$$

3.0 RESULTS AND DISCUSSION

Figure 3 plots the temperature profile for the inlet and outlet flue gas temperature. Due to the deactivation of 4 tubes, a higher inlet gas temperature (or greater inlet enthalpy) is needed to achieve a similar range of outlet gas temperature. For example, before the tube deactivation (2014 data), the inlet gas temperature is required to achieve an outlet gas temperature range between 338 °C and 349 °C which is 490 °C to 512 °C. However, due to the decrease in surface heating area caused by the tube deactivation in 2017, the inlet gas temperature needs to be increased from 512 °C to 525 °C. This

is a 2.5% to 7.0% increase in inlet gas temperature requirement, or a 0.6% to 1.8% inlet gas temperature (enthalpy) increase required for every tube deactivated.

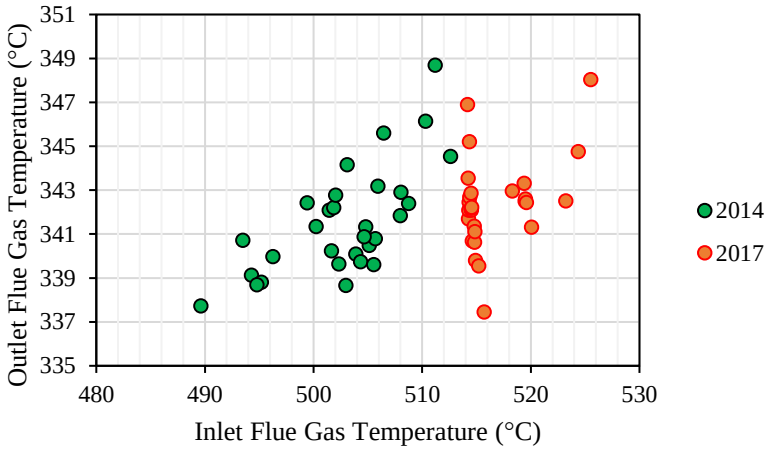

Figure 3. Average inlet temperature of flue gas is higher in 2017 compared to 2014

Table 4 compares the average steam temperatures between 2014 and 2017. At an approximately similar inlet steam temperature, the average increase in steam temperature was reduced by 6%. This is lower than the designed operating temperature of 387 °C which could affect the subsequent process. Figures 4 and 5 show the direct effects of tube deactivation on the achievable steam temperature differences. Figure 4 shows that the 2017 superheater produces a lower steam temperature difference while having a larger flue gas temperature drop compared to the 2014 superheater. Evidently, the superheater could generate a higher rate of heat transfer at a specific flue gas temperature difference and steam flow rate before the tubes are deactivated, as a direct result of a significant reduction in heating area.

In 2014, prior to the tube deactivation, a flue gas temperature difference of 150 °C to 170 °C could increase the steam temperature by 129 °C to 143 °C. However, the 2017 superheater could only achieve a steam temperature increase by 118 °C to 133 °C even when the flue gas temperature difference is approximately 10-20% larger. In heat transfer science, a larger change in the heat source temperature (flue gas) should be translated to a higher temperature increase of the heat sink temperature (steam). However, the temperature change of the heat sink fluid is also dependant on the flow rate. Therefore, the decision of the plant engineers to increase the steam flow rate due to tube plugging has caused a lower steam quality to be produced. Also, the reduction in heating area caused a lower steam temperature increase even though the flue gas temperature difference was higher, indicating that the superheater effectiveness has been reduced.

The reduction in superheater effectiveness is also seen through the profiles of steam temperature difference relative to the steam flow rate (Figure 5). At similar flow rates, the mean steam temperature increase for the 2014 superheater is higher than the 2017 superheater. Comparing the increase in steam temperatures, the mean steam temperature difference between the 2014 and 2017 superheaters is 8.7 °C. Generally, the deactivation of the tubes led to an average reduction of 6.4% in the achievable steam temperature difference at a similar steam flow rate.

The effectiveness of the superheater is partly influenced by the heat exchanger area (heating surface). Figure 6 shows that the effectiveness of the superheater was higher in 2014 than in 2017. In 2014, the effectiveness ranged between 0.51 and 0.56. The effectiveness dropped to a range of 0.44 to 0.49 after the tube deactivation, even when the steam flow rate was increased to offset the heating surface reduction factor. The sensitivity of the superheater to the available surface area is evident.

As a direct comparison, the effectiveness of the superheater in 2014 and 2017 was observed to be 0.51 and 0.45 respectively, at a similar design with a steam flow rate of 80 tonnes/hour. Relatively, the effectiveness of the superheater in 2014 averages at 0.54, while the average effectiveness for year 2017 is 0.48. It can be concluded that the decrease in heating surface area is more dominant than the impact of the steam mass flow rate on the effectiveness of the superheater. This might be caused by the limitations in heat transfer per mass of steam due to its vapour phase.

Table 4. Details of steam temperature at the superheater

Service Year	Average Inlet Steam Temperature (°C)	Average Outlet Steam Temperature (°C)	Average Temperature Increase (°C)
2014	250.5	386.1	135.5
2017	248.2	376.3	128.1

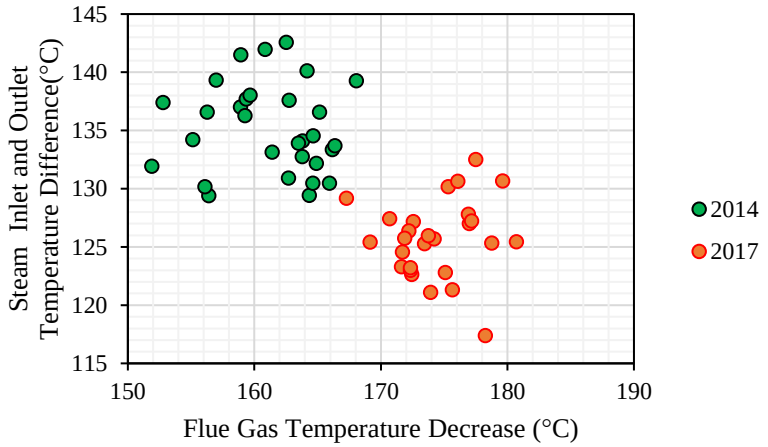

Figure 4. Profile of the steam temperature increase relative to the flue gas temperature decrease

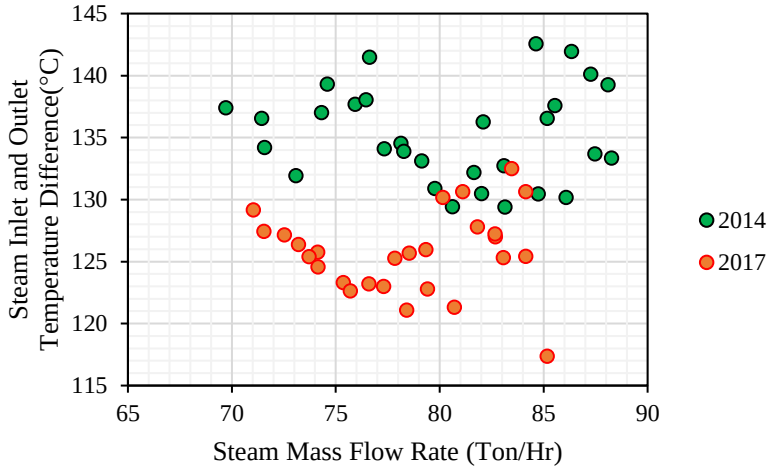

Figure 5. Effect of mass flow rate of steam on the steam inlet and outlet temperature difference

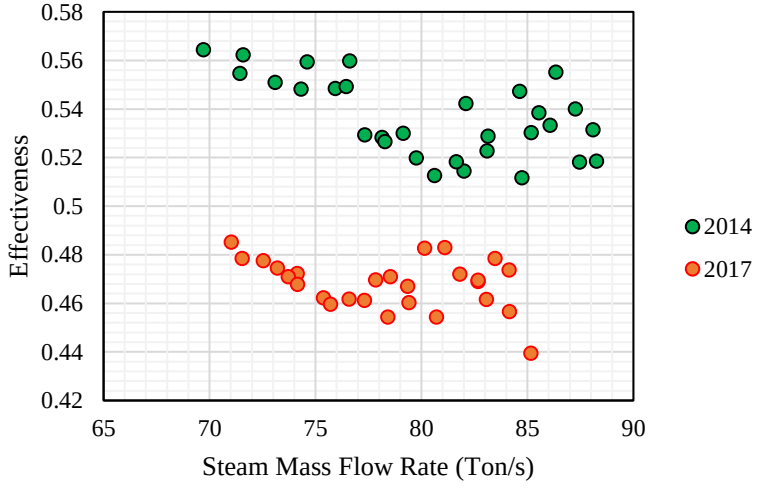

Figure 6. Effect of mass flow rate of steam on the effectiveness of the superheater heat exchanger

4.0 CONCLUSION

During the operation of a steam superheater in a petrochemical plant, the tubes will suffer from corrosion effects, and it becomes necessary to plug all the defective tubes. The extent of the tube deactivation on the operational performance of the superheater was objectively studied through the application of temperature profiling and first law thermodynamics analysis. To achieve the required range of steam output temperature, the enthalpy of the inlet gas must be increased by 0.6% to 1.8% for each tube deactivated. At a similar steam flow rate, a reduction between 6.0% to 6.4% is expected to the achievable steam temperature increase due to the deactivation of the four superheater tubes. Further reduction of active surface heating area would result in process interruption as the subsequent process require the steam temperature to be at

387 °C. This warrant for the superheater replacement before further tube deactivation due to tube failure occurrence. An average difference in effectiveness of approximately 11% was also identified due to the tube deactivation. Based on these major observations, the negative effects of the tube deactivation on the superheater performance is evident and attempting to offset the effects by increasing the steam flow rate is not a viable solution due to the limitations in gas-to-gas heat transfer mechanisms.

5.0 ACKNOWLEDGEMENT

The authors would like to thank the management and engineering staff of Petronas Chemical Methanol Sdn. Bhd. for the support and assistance during the project.

6.0 NOMENCLATURE

$\dot{m}_c$	Steam Mass Flow Rate (Ton/hr)
T_c	Inlet and Outlet Temperature of Steam (°C)
$c_{p,c}$	Steam Specific Heat Capacity (J/kg.K)
$\dot{m}_h/\dot{m}_{flue\ gas}$	Flue Gas Mass Flow Rate (Ton/hr)
T_h	Inlet and Outlet Temperature of Flue Gas (°C)
$c_{p,h}$	Flue Gas Specific Heat Capacity (J/kg.K)
$\dot{V}$	Natural and Mixture Gas Inlet Volume Flow Rate (Nm^3/hr)
$\dot{V}_{air}$	Combustion Air Inlet Volume Flow Rate (Nm^3/hr)
M	Molecular Weight Gas (kg/K.mol)
M_{air}	Molecular Weight Combustion Air (mole percent)
$c_{p,C}$	Carbon dioxide specific heat capacity (J/kg.K)
T_{pr}	Pseudo Reduced Temperature (K)
P_{pr}	Pseudo Reduced Pressure (MPa)
T_{pc}	Pseudo Critical Temperature (K)
P_{pc}	Pseudo Critical Pressure (MPa)

7.0 REFERENCES

[1] M. F. Remeli, L. Tan, A. Date, B. Singh, and A. Akbarzadeh, "Simultaneous power generation and heat recovery using a heat pipe assisted thermoelectric generator system," *Energy Conversion and Management*, vol. 91, pp. 110–119, 2015.

[2] S. H. Symoens *et al.*, "State-of-the-art of coke formation during steam cracking: Anti-coking surface technologies," *Industrial Engineering Chemical Research*, vol. 57, no. 48, pp. 16117–16136, 2018.

[3] S. O. Oyedepo and B. A. Fakeye, "Waste heat recovery technologies: Pathway to sustainable energy development," *Journal of Thermal Engineering*, vol. 7, no. 1, pp. 324–348, 2021.

[4] Y. Han, H. Wu, Z. Geng, Q. Zhu, X. Gu, and B. Yu, "Review: Energy efficiency evaluation of complex petrochemical industries," *Energy*, vol. 203, pp. 117893, 2020.

[5] Y. V. Shatskikh, A. I. Sharapov, and I. G. Byankin, "Analysis of deep heat recovery from flue gases," in *Journal of Physics: Conference Series*, vol. 891, no. 1, pp. 012188, 2017.

[6] E. Woolley, Y. Luo, and A. Simeone, "Industrial waste heat recovery: A systematic approach," *Sustainable Energy Technology Assessments*, vol. 29, pp. 50–59, 2018.

[7] D. Gewald, K. Siokos, S. Karellas, and H. Spliethoff, "Waste heat recovery from a landfill gas-fired power plant," *Renewable and Sustainable Energy Reviews.*, vol. 16, no. 4, pp. 1779–1789, 2012.

[8] T. Blumberg, T. Morosuk, and G. Tsatsaronis, "Exergy-based evaluation of methanol production from natural gas with CO_2 utilization," *Energy*, vol. 141, pp. 2528–2539, 2017.

[9] O. J. Khaleel, T. K. Ibrahim, F. B. Ismail, and A. T. Al-Sammarraie, "Developing an analytical model to predict the energy and exergy-based performances of a coal-fired thermal power plant," *Case Studies in Thermal Engineering.*, vol. 28, p. 101519, 2021.

[10] I. Johnson, W. T. Choate, and A. Davidson, "Waste heat recovery: Technology and opportunities in U.S. industry," Boston, Mar. 2008. [online] Available: https://www.osti.gov/servlets/purl/1218716.

[11] M. Granda, M. Trojan, and J. Taler, "CFD analysis of steam superheater, transient state," in *E3S Web of Conferences*, vol. 128, p. 04009, 2009.

[12] J. Purbolaksono, J. Ahmad, L. C. Beng, A. Z. Rashid, A. Khinani, and A. A. Ali, "Failure analysis on a primary superheater tube of a power plant," *Engineering Failure Analysis*, vol. 17, no. 1, pp. 158–167, 2010.

[13] R. K. Roy, S. K. Das, A. K. Panda, and A. Mitra, "Analysis of superheater boiler tubes failed through non-linear heating," in *Procedia Engineering*, vol. 86, pp. 926–932, 2014.

[14] G. K. Gupta and S. Chattopadhyaya, "Critical failure analysis of superheater tubes of coal-based boiler," *Strojniski Vestnik Journal of Mechanical Engineering*, vol. 63, no. 5, pp. 287–299, 2017.

[15] A. Movahedi-Rad, S. S. Plasseyed, and M. Attarian, "Failure analysis of superheater tube," *Engineering Failure Analysis*, vol. 48, pp. 94–104, 2015.

[16] P. Madejski and D. Taler, "Analysis of temperature and stress distribution of superheater tubes after attemperation or sootblower activation," *Energy Conversion and Management*, vol. 71, pp. 131–137, 2013.

[17] A. Sadeghianjahromi and C. C. Wang, "Heat transfer enhancement in fin-and-tube heat exchangers – A review on different mechanisms," *Renewable and Sustainable Energy Reviews*, vol. 137, 2021.

[18] W. Zima, "Simulation of steam superheater operation under conditions of pressure decrease," *Energy*, vol. 172, pp. 932–944, 2019.

[19] I. H. Aljundi, "Energy and exergy analysis of a steam power plant in Jordan," *Applied Thermal Engineering*, vol. 29, no. 2–3, pp. 324–328, 2009.

[20] S. Kumar, D. Kumar, R. A. Memon, M. A. Wassan, and S. A. Mir, "Energy and exergy analysis of a coal fired power plant," *Mehran University Research Journal in Engineering and Technology.*, vol. 37, no. 4, pp. 611–624, 2018.

[21] J. Clay and J. Mathias, "Energetic and exergetic analysis of a multi-stage turbine, coal-fired 173 MW power plant," *International Journal of Exergy*, vol. 27, no. 4, pp. 419–436, 2018.

[22] M. Elhelw, K. S. Al Dahma, and A. el H. Attia, "Utilizing exergy analysis in studying the performance of steam power plant at two different operation mode," *Applied Thermal Engineering*, vol. 150, pp. 285–293, 2019.

[23] N. Bianco, A. Fragnito, M. Iasiello, and G. Maria Mauro, "A comprehensive approach for the multi-objective optimization of Heat Recovery Steam Generators to maximize cost-effectiveness and output power," *Sustainable Energy Technologies Assessment*, vol. 45, p. 101162, 2021.

[24] S. Begum, A. N. M. Karim, A. S. M. Zamani, and M. A. Shafii, "Wall Thinning and Creep Damage Analysis in Boiler Tube and Optimization of Operating Conditions," *Journal of Mechatronics*, vol. 1, pp. 1–6, 2013.

[25] A. Saha, H. Roy, and A. K. Shukla, "Failure Investigation of a Final Super Heater Tube in a 140 MW Thermal Power Plant," *Case Studies in Engineering Failure Analysis*, vol. 15, no. 2, pp. 184–189, 2015.

[26] J. Ahmad, J. Purbulaksono, L. C. Beng, A. Z. Rashid, A. Khinani, and A. A. Ali, "Failure investigation on rear water wall tube of boiler," *Engineering Failure Analysis*, vol. 16, no. 7, pp. 2325–2332, 2009.

[27] M. Botha and M. P. Hindley, "One-way Fluid Structure Interaction modelling methodology for boiler tube fatigue failure," *Engineering Failure Analysis*, vol. 48, pp. 1–10, 2015.

[28] D. Šeruga, M. Fajdiga, and M. Nagode, "Creep damage calculation for thermo mechanical fatigue," *Strojniski Vestnik Journal of Mechanical Engineering*, vol. 57, no. 5, pp. 371–378, 2011.

[29] A. Saha and A. K. Shukla, "Failure of a Secondary Superheater Tube in a 140-MW Thermal Power Plant," *Journal of Failure Analysis and Prevention*, vol. 14, no. 1. pp. 10–12, 2014.

[30] American Society of Mechanical Engineers, *ASME Boiler and Pressure Vessel Code: I Rules for Construction of Power Boilers*, 2013th ed. New York: ASME, 2013.

[31] A. Hafid, M. Pancoko, and S. Pujiarta, "Analysis of the number of minimum tubes for optimal operation in a heat exchanger RSG G.A. Siwabessy," in *Prosiding Seminar Nasional Teknologi Energi Nuklir*, 2016, pp. 625–632.

[32] R. B. Bird, W. E. Stewart, and E. N. Lightfoot, *Transport Phenomena*. Madison: John Wiley & Sons Inc, 2002.

[33] Y. A. Çengel, M. A. Boles, and M. Kanoğlu, *Thermodynamics: An Engineering Approach, Ninth Edition*. McGraw-Hill Education, 2019.

[34] O. Nematollahi and K. C. Kim, "Real-gas effects: The state of the art of organic Rankine cycles," *Journal of Cleaner Production*, vol. 277, p. 124102, 2020.

[35] E. Sanjari and E. N. Lay, "An accurate empirical correlation for predicting natural gas compressibility factors," *Journal of Natural Gas Chemistry*, vol. 21, no. 2, pp. 184–188, 2012.

[36] J. Ren, F. Yang, D. Ma, G. Le, and J. Zhong, "Pneumatic performance study of a high-pressure ejection device based on real specific energy and specific enthalpy," *Entropy*, vol. 16, no. 9, pp. 4801–4817, 2014.

[37] C. Coskun, Z. Oktay, and N. Ilten, "A new approach for simplifying the calculation of flue gas specific heat and specific exergy value depending on fuel composition," *Energy*, vol. 34, no. 11, pp. 1898–1902, 2009.

[38] Y. A. Cengel, *Heat Transfer: A Practical Approach*, 2nd Edition. New York: McGraw-Hill, 2002. [Online]. Available: www.LearnEngineering.in